Scientific Research Publishing

Open Journal of Applied Sciences, 2026, 16(6), 2138-2151
https://www.scirp.org/journal/ojapps
ISSN Online: 2165-3925
ISSN Print: 2165-3917

# Modeling of the TEC during Periods of Quiet Geomagnetic Activity at the Niamey GPS Station during Cycle 24

**Wambi Emmanuel Sawadogo[1,2*], Inza Gnanou[1,2], Moussa Sankara[1], Doua Allain Gnabahou[1], Boukar Makinta[3], Frédéric Ouattara[1]**

[1]Laboratory of Analytical Chemistry, Space and Energetic Physics (L@CAPSE), Norbert Zongo University (UNZ), Koudougou, Burkina Faso
[2]Interdisciplinary Laboratory for Research in Applied Sciences (LIRSA), Higher Normal School (ENS), Ouagadougou, Burkina Faso
[3]Laboratoire d'Energie, d'Electronique, d'Automatisme et d'Informatique Industrielle (L3EA2I), Université Abdou Moumouni, Niamey, Niger
Email: *sawwemma1@yahoo.fr

**How to cite this paper:** Sawadogo, W.E., Gnanou, I., Sankara, M., Gnabahou, D.A., Makinta, B. and Ouattara, F. (2026) Modeling of the TEC during Periods of Quiet Geomagnetic Activity at the Niamey GPS Station during Cycle 24. *Open Journal of Applied Sciences*, **16**, 2138-2151.
https://doi.org/10.4236/ojapps.2026.166120

**Received:** May 19, 2026
**Accepted:** June 12, 2026
**Published:** June 15, 2026



## Abstract

The IRI-2020 model predicts the presence of intense counter-electrojet at the Niamey equatorial station during periods of quiet geomagnetic activity, across different solar cycle phases and seasons. Generally, Total Electron Content (TEC) variability exhibits a trough at dawn and a rapid increase after sunrise, reaching a peak in the afternoon. This is explained by the decrease in photoionization during the night and an increase in recombination. After sunrise, the intensification of solar radiation increases photoionization, causing a rapid increase in the TEC until the local afternoon peak. After sunset, the TEC decreases due to the reduction in photoionization and the strengthening of recombination. The IRI model indicates, as expected, that ionization increases with sunspot activity. Indeed, the TEC is maximal during the maximum phase and minimal during the minimum phase. Since the variation in the number of sunspots is positive during the ascending phase and negative during the descending phase, TEC values are higher during the ascending phase than during the descending phase. The seasonal variation of the TEC shows a semi-annual anomaly, meaning greater ionization at the equinoxes than at the solstices. Autumn values are higher than spring values, and winter values are higher than summer values. The IRI-2020 prediction indicates a nighttime winter anomaly from 2100 LT until dawn. The comparative study between the predictions of the NeQuick2 model and the reference IRI model shows considerable discrepancies during the day. However, at night, the two models pre-

sent similar estimates.

## Keywords

Total Electron Content (TEC), Quiet Geomagnetic Activity, IRI-2020, NeQuick2

## 1. Introduction

Total Electron Content (TEC) is an important ionospheric parameter used to monitor possible space weather impacts on satellite to ground communication and satellite navigation system [1]. Studying the variability of this parameter is therefore crucial. TEC measurements from ionospheric observatories are often scarce in some regions, making modeling projects highly beneficial. Both IRI and NeQuick models are classical empirical ionospheric models, which are widely used for ionospheric variability characterization and assessment, and provide effective alternatives for areas with limited ionospheric observatories [2]. The IRI project, sponsored by the Committee on Space Research (COSPAR) and the International Union of Radio Science (URSI), was launched in 1968. It produced an empirical climatological ionospheric model based on both ground-based and space-based observations of the ionosphere collected over the past decades on a global basis. Since April 2014, IRI has been recognized as the official standard for the ionosphere by the International Standardization Organization (ISO) [3]. NeQuick2 is the latest version of the NeQuick ionosphere electron density model developed at the Aeronomy and Radiopropagation Laboratory (now T/ICT4D Laboratory) of the Abdus Salam International Centre for Theoretical Physics (ICTP)-Trieste, Italy with the collaboration of the Institute for Geophysics, Astrophysics and Meteorology of the University of Graz, Austria [4].

In this study, we investigated the TEC variability at the Niamey station in Niger (Geo Lat 13˚28'45.3"N; Geo Long: 02˚10'59.5"E). Lacking ground-based measurements, we used the latest versions of the IRI and NeQuick models, namely IRI-2020 and NeQuick2, to analyse their predictions. Our research station is located at the trough of the equatorial ionization anomaly (EIA). The formation of the EIA can influence the diurnal and seasonal variability of the TEC. Its variability is also linked to 11-year solar cycle [5]-[9]. To address this, we focused on modeling the diurnal variability of the TEC by solar phase and by season.

In the second section of our work, we present the data and methodology used. The third section deals with the results, followed by a discussion, and the fourth section is devoted to the synthesis of the document.

## 2. Data and Methodology

In this section we will present the data used for this work as well as the methodology used.

### 2.1. Data

In this study, we used the TEC parameter estimated at the Niamey Station (Geo Lat 13˚28'45.3"N; Geo Long: 02˚10'59.5"E) by the IRI-2020 and NeQuick 2 models for the period from 2008 to 2018, covering solar cycle 24. The IRI-2020 and NeQuick 2 models are available at https://kauai.ccmc.gsfc.nasa.gov/instantrun/iri/ and https://t-ict4d.ictp.it, respectively.

Solar and geomagnetic activity are two major factors affecting ionospheric density. To account for these activities, we also used data such as the sunspots number Rz and the average Aa values of the geomagnetic index aa available at websites http://omniweb.gsfc.nasa.gov/form/dx1.html and http://www.isgi.unistra.fr/indices_aa.php respectively.

### 2.2. Methodology Used

- **Determination of solar cycle phases**

We used the cutting proposed by [10]. **Table 1** shows the periods of the different phases of the solar cycle 24.

**Table 1.** Distribution of years in cycle 24 by solar phase.

| Solar cycle phase | Years |
|---|---|
| Minimum | 2008-2009 |
| Ascending | 2010-2011 |
| Maximum | 2012-2014 |
| Descending | 2015-2018 |

- **Distribution of the seasons**

**Table 2** shows the cutting of the seasons by month.

**Table 2.** Cutting of the seasons

| Seasons | Months |
|---|---|
| Winter | December-January-February |
| spring | March-April-May |
| Summer | June-July-August |
| Autumn | September-October-November |

- **Selection of quiet days**

According to the classification of [11] revised by [12] which we used, days of quiet geomagnetic activity correspond to days where the daily mean values of Aa are less than 20 nT. **Table 3** gives the number of quiet days per year.

- **Method for analyzing the variability of the TEC**

Based on the modeled TEC values, we plotted hourly profiles according to solar phases and seasons. TEC is expressed in units of tecu (1 tecu = $10^{16}$ electrons per

**Table 3.** Number of quiet days for each year of cycle 24.

| Years | 2008 | 2009 | 2010 | 2011 | 2012 | 2013 | 2014 | 2015 | 2016 | 2017 | 2018 |
|---|---|---|---|---|---|---|---|---|---|---|---|
| Number of quiet days | 271 | 345 | 305 | 278 | 259 | 273 | 270 | 199 | 212 | 230 | 276 |

square meter). The IRI-2020 model was first used for seasonal and phase predictions. Then, we simultaneously plotted the predictions of IRI-2020 and NeQuick2 for a comparative study of the variabilities proposed by the two models. It should be noted that Local Time (LT) is one hour ahead of Universal Time (UT). From a morphological perspective, the profiles are analyzed based on the profile types of [13] in the equatorial region.

For a quantitative analysis, we used the following quantities:

1) the relative gap between the TEC values of the equinox months (spring and autumn)

$\delta_{eq} = \frac{(TEC)_{spring} - (TEC)_{autumn}}{(TEC)_{spring}} \times 100$ . If $|\delta_{eq}| > 10\%$ we have an equinoxial asymmetry.

2) the relative gap between the TEC values of solstice months (winter and summer)

$\delta_{sol} = \frac{(TEC)_{Winter} - (TEC)_{Summer}}{(TEC)_{hiver}} \times 100$ . If $\delta_{sol} > 10\%$ , we have a winter anomaly.

3) the relative gap between the IRI-2020 and NeQuick2 predictions

$$\delta_{IRI\text{-}NeQ} = \frac{(TEC)_{IRI\text{-}2020} - (TEC)_{NeQuick2}}{(TEC)_{IRI\text{-}2020}} \times 100$$

If $\delta_{IRI\text{-}NeQ} > 10\%$ , IRI-2020 overestimates the TEC compared to NeQuick2.
If $\delta_{IRI\text{-}NeQ} < 10\%$ , IRI-2020 underestimates the TEC compared to NeQuick2.
For $|\delta_{IRI\text{-}NeQ}| \leq 10\%$ , Both models make almost the same prediction of the TEC.

## 3. Results and Discussion

This section presents the results of the IRI-2020 modeling of the TEC as a function of solar phases and seasons. A comparative study is also conducted between the predictions of IRI-2020 and NeQuick2. These results are followed by a discussion.

### 3.1. Diurnal Variation of the TEC by Solar Phase

The IRI-2020 modeling of the TEC yields "reversed" profiles during all phases (**Figure 1**). Indeed, a minimum TEC value is observed at 0500LT, followed by a rapid increase until 1600LT, where maximum values are observed. **Table 4** shows the TEC extrema for each solar phase. After 1600LT, the TEC decreases until nightfall. Later in the night, the TEC continues to decrease until morning at 0500LT. Higher ionization is recorded at solar maximum and lower ionization at

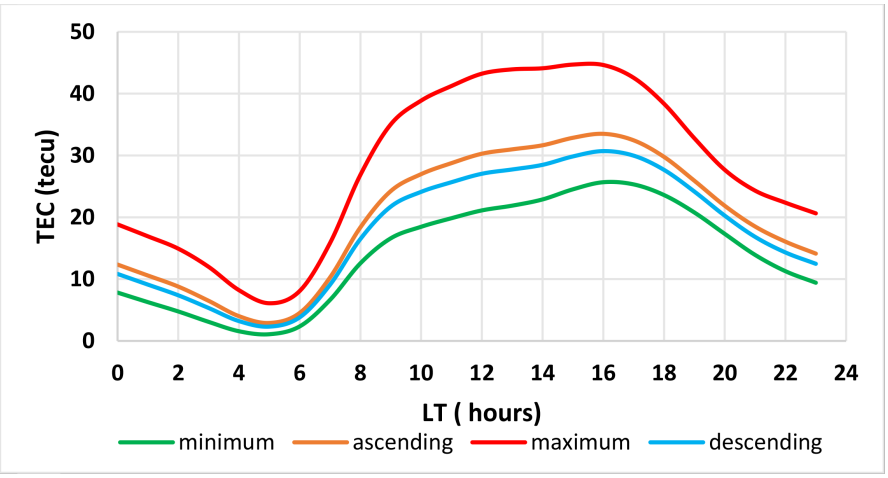


**Figure 1.** IRI-2020 prediction of the hourly variation of the TEC by solar phase.

**Table 4.** TEC extrema by solar phase.

| Phase | TEC pick value | | TEC minimum value | |
|---|---|---|---|---|
| | Value (tecu) | Time (LT) | Value (tecu) | Time (LT) |
| Minimum | 25.67 | 16:00 | 1.08 | 05:00 |
| Ascending | 33.49 | 16:00 | 2.90 | 05:00 |
| Maximum | 44.63 | 16:00 | 6.09 | 05:00 |
| Descending | 30.71 | 16:00 | 2.31 | 05:00 |

solar minimum, such that: $TEC_{Max} > TEC_{Asc} > TEC_{Desc} > TEC_{Min}$. Ionization increases with the intensity of solar activity. During the phase maximum (2012-2014), the number of sunspots is at its highest, thus implying an increase in the TEC during this period. The number of sunspots varies positively during the ascending phase, while it shows a negative variation during the descending phase. This explains the relatively higher TEC values during the ascending phase compared to the descending phase. The "Reversed" type profile, according to [14], indicates the presence of an intense counter-electrojet. Given the position of our study station (the EIA trough), we could expect the signature of the ExB vertical drift that is to say, a "noon bite out" profile. However, [15] showed that the TEC profiles during quiet periods at this station do not highlight the effect of ExB drift at local noon. [16] used the CODG TEC from IGS (International GNSS Service) database to study TEC variability at the Niamey station. They showed that the TEC exhibits a minimum at 05:00 LT and a rapid increase with sunrise, reaching a maximum in the local afternoon. They argue that the trough observed at dawn reflects a decrease in nighttime photoionization and an increase in recombination phenomenon during quiet periods. [17] cited by [16] showed that in the northern ridge of the Indian equatorial ionization anomaly, a trough appears between 05:00LT and 06:00LT, and the TEC increases at sunrise, reaching a peak in the afternoon between 13:00LT and 16:00LT, followed by a gradual decrease after sun-

set. The rapid increase after sunrise is related to Extreme UltraViolet (EUV) radiation and the upward vertical drift ExB [17] [18].

### 3.2. Seasonal Variation of the TEC

Figure 2 provides a seasonal prediction of the TEC using the IRI-2020 model. Panel (a) shows the variation of the TEC according to the different seasons, and panel (b) shows the variation of the mean TEC values during the equinox and solstice seasons.

The seasonal profiles are of the reversed type. From sunrise (05:00 LT) until 16:00 LT, ionization is higher in autumn (maximum TEC value: 38.26 tecu) and lower in summer (maximum TEC value: 30.66 tecu). The order of the TEC values is: $TEC_{Aut} > TEC_{Spring} > TEC_{Win} > TEC_{Sum}$. The seasonal variations of the TEC generally show higher ionization at the equinoxes than at the solstices. Indeed, according to panel (a), from sunrise (05:00LT) until 21:00LT, the TEC values in spring and autumn are higher than those in winter and summer. Compared to other seasons, a notable decrease in TEC is observed in summer, from 21:00LT (14.36 tecu) until dawn at 04:00LT (2.44 tecu). During this season, the maximum value occurs later, at 17:00 LT, with 30.66 tecu. Panel (b) clearly shows that the TEC at the equinoxes is always higher than the solstice values ($TEC_{Equinoxe} > TEC_{Solstice}$). The IRI-2020 model predicts maximum ionization at the equinoxes and minimum ionization at the solstices. This type of TEC variation is well known as the semi-annual anomaly [19]-[24]. This anomaly could be explained by an increase in the thermospheric atom-to-molecule ratio [O/N2], resulting in a higher electron density. The high relative ionization during the equinoxes can be explained by the fact that during this period the sun is overhead the equator [25]. During the solstices, the tilt of the Earth's rotational axis moves the equatorial zone away from the sun, promoting a decrease in ionization.

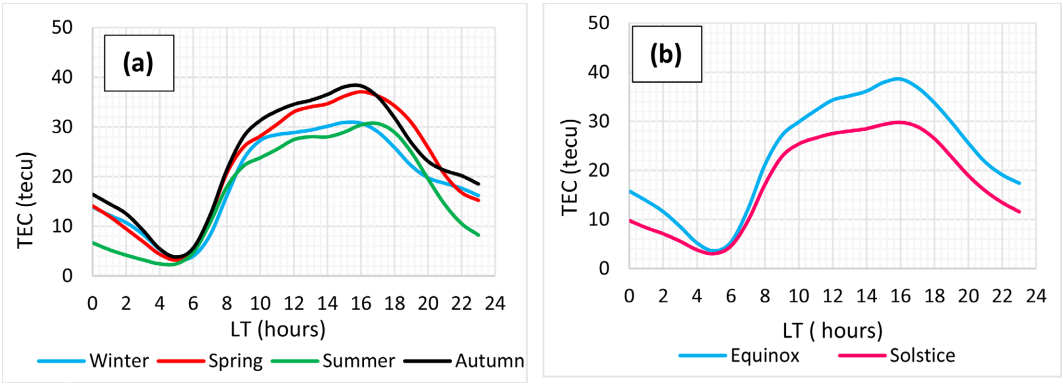


Figure 2. IRI-2020 prediction of the seasonal variation of the TEC.

Figure 3 represents the IRI-2020 prediction of the hourly variation of the TEC at the equinoxes and solstices. Panel (a) shows the variation of the TEC in spring (March-April) and autumn (December-January), as well as the relative difference ($\delta_{eq}$) between the values for these equinox seasons. Panel (b) shows the variation

of the TEC in winter (December-January) and summer (June-July), as well as the relative difference ( $\delta_{sol}$ ) between the values for these solstice seasons.

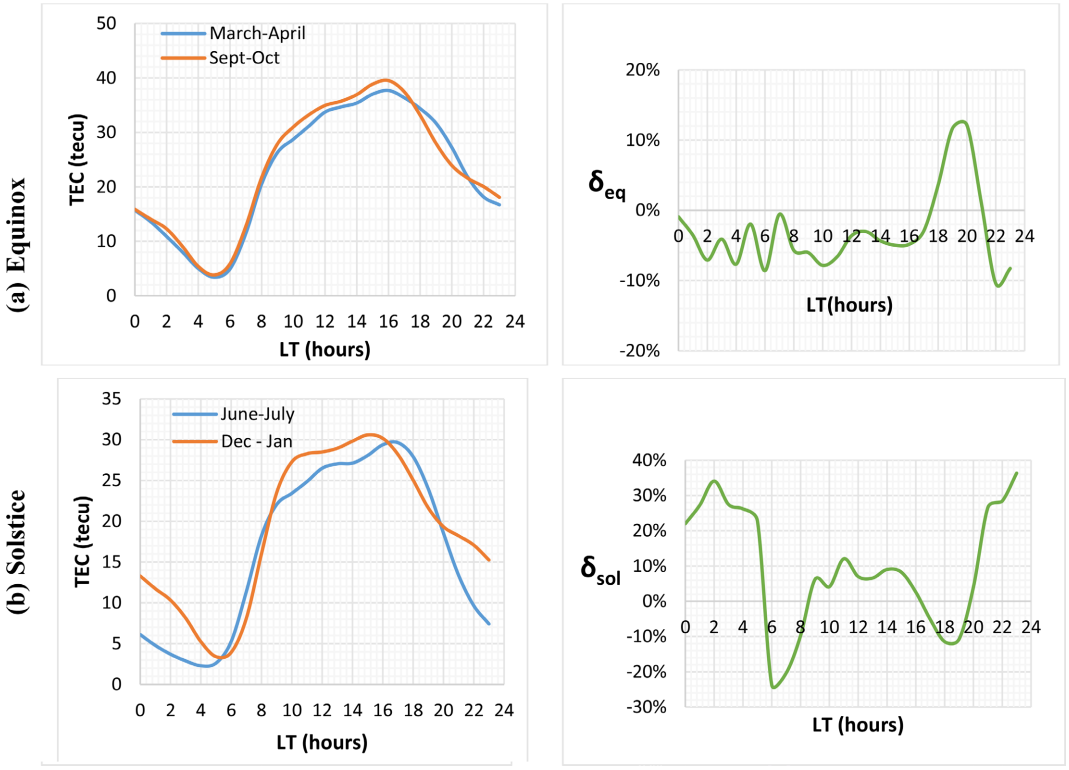


**Figure 3.** Modeling the diurnal variation of the TEC at equinoxes and solstices using IR-2020.

The TEC values are practically identical in spring (March-April) and autumn (September-October), with $|\delta_{eq}| < 10\%$ at all hours except 19:00 LT and 20:00 LT, with relative differences of 11.67% and 12.13%, respectively. The IRI model shows almost no equinoctial asymmetry during the quiet activity. In the equatorial region, between 19:00 LT and 20:00 LT, the pre-reversal phenomenon occurs, causing nighttime peaks in TEC variation [26]-[28]. IRI does not predict this phenomenon but indicates a significant gap between spring and autumn values. Regarding the solstice variation, during the night from 21:00LT until dawn (05:00LT), the TEC values during winter are higher than those during summer, with the relative difference $\delta_{sol}$ between 22.16% and 34.27%. This reflects a nocturnal winter anomaly. The seasonal variation in the neutral thermospheric composition has been suggested as the main source of this winter anomaly [29]-[31].

### 3.3. Comparison of the IRI-2020 and the NeQuick2 Model

The IRI model The IRI model has become the official standard for the ionosphere by the International Standardization Organization (ISO) [3], in this section, we propose to use another model (NeQuick2) to compare its predictions.

- **Predictions of both models based on solar phases**

Figure 4 shows, for each phase, the hourly TEC profiles predicted by both

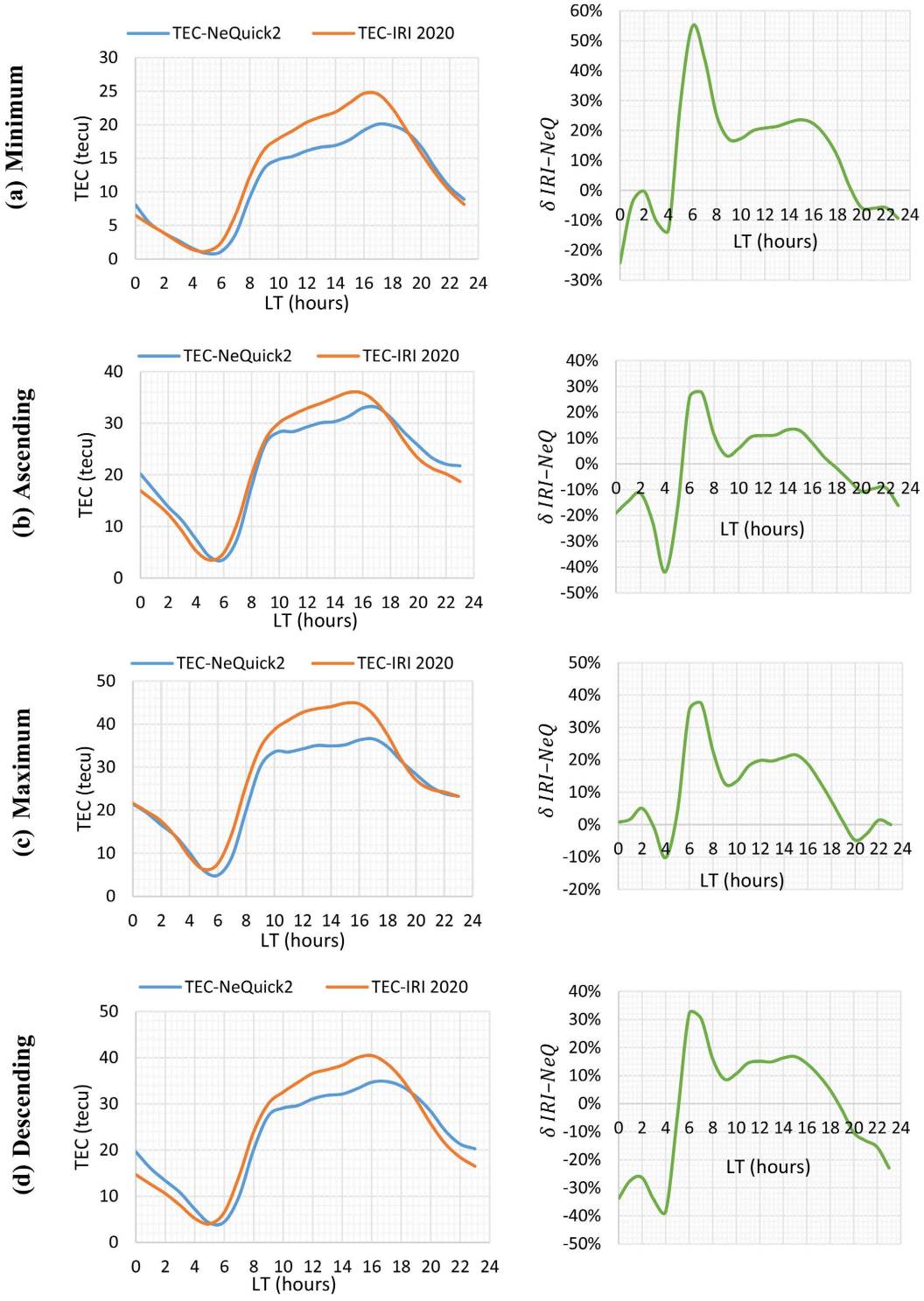


**Figure 4.** Diurnal variations of the TEC by IRI-2020 and NeQuick2 as a function of solar phases.

models, as well as the relative difference $\delta_{\text{IRI-NeQ}}$ between the two predictions.

From a morphological point of view, the two models have the same trend in all phases of the solar cycle, with a "reversed" profile. They therefore predict the same electrodynamic behavior of the ionosphere, notably the intense counter-electro-

ject [14].

At solar minimum, IRI-2020 overestimates the TEC compared to NeQuick2 between 05:00LT and 18:00LT with $\delta_{\text{IRI-NeQ}} > 10\%$. A maximum value is recorded at 06:00LT with a 55.10% relative difference. After nightfall, the two models have approximately the same prediction from 19:00LT to 23:00LT and from 01:00LT to 04:00LT. A brief underestimation of IRI is noted at 00:00LT with a −24.06% relative difference. During the ascending phase, IRI-2020 overestimates the TEC in the morning from 05:00LT to 08:00LT and from 11:00LT to 15:00LT. After 16:00LT until 22:00LT, the two models give essentially the same TEC predictions. From 00:00LT to 05:00LT, an underestimation of IRI is noted. Particularly at 04:00LT, the relative discrepancy is −42.21%. At the maximum phase, IRI-2020 overestimates the TEC during the day from 06:00LT to 17:00LT, with a maximum $\delta_{\text{IRI-NeQ}}$ value of 37.19% at 07:00LT. After 18:00LT until 05:00LT, $\left|\delta_{\text{IRI-NeQ}}\right| < 10\%$; the two models present almost identical estimates during the night. During the descending phase, IRI-2020 overestimates from 06:00LT to 17:00LT, with a maximum discrepancy of 32.09 % at 06:00LT. In the evening, from 18:00LT to 20:00LT, the predictions are almost identical for both models. Between 21:00LT and 04:00LT, the IRI model underestimated NeQuick2, with the largest gap of −38.17% at 04:00LT.

From a quantitative perspective, IRI-2020 generally overestimates the TEC during the day compared to NeQuick2. Both models present similar predictions during the night, except during the descending phase starting at 21:00LT. Except during the descending phase, modeling is more satisfactory at night than during the day throughout all solar phases. The modeling difficulties during the day are likely related to the significant variability of ionization. Furthermore, the models exhibit considerable prediction discrepancies at dawn, when photoionization is rapidly triggered by the first solar radiation.

- Predictions of both models based on the seasons

**Figure 5** shows the seasonal variations of the TEC predicted by the two models, as well as the relative difference $\delta_{\text{IRI-NeQ}}$ between the two predictions.

Both models exhibit the same morphological trends in all seasons, with a reversed profile. They therefore predict the same electrodynamic behavior of the ionosphere, notably the intense counter-electroject [14].

In winter, quantitative analysis shows an overestimation of IRI-2020 at all times except from 18:00 to 20:00, when the two models have almost identical TEC predictions. The maximum value of $\delta_{\text{IRI-NeQ}}$ is 42.30%, recorded at 07:00. In spring, IRI overestimates the TEC at the beginning of the day between 06:00 LT and 08:00 LT, with a maximum relative difference of 29.41% at 07:00 LT. From 09:00LT onwards, the two models predict similar values until nightfall at 23:00 LT. From 00:00 LT until 05:00 LT, IRI-2020 underestimates the TEC, with a large gap of −71.08% at 04:00 LT. In summer, IRI-2020 overestimates the TEC during the day from 05:00 LT to 18:00 LT, with a maximum discrepancy of 43.19% at 06:00 LT. During the night from 19:00 LT until dawn, IRI underestimates the TEC compared to NeQuick, with a maximum discrepancy of −50.04% at 00:00 LT. In autumn, the

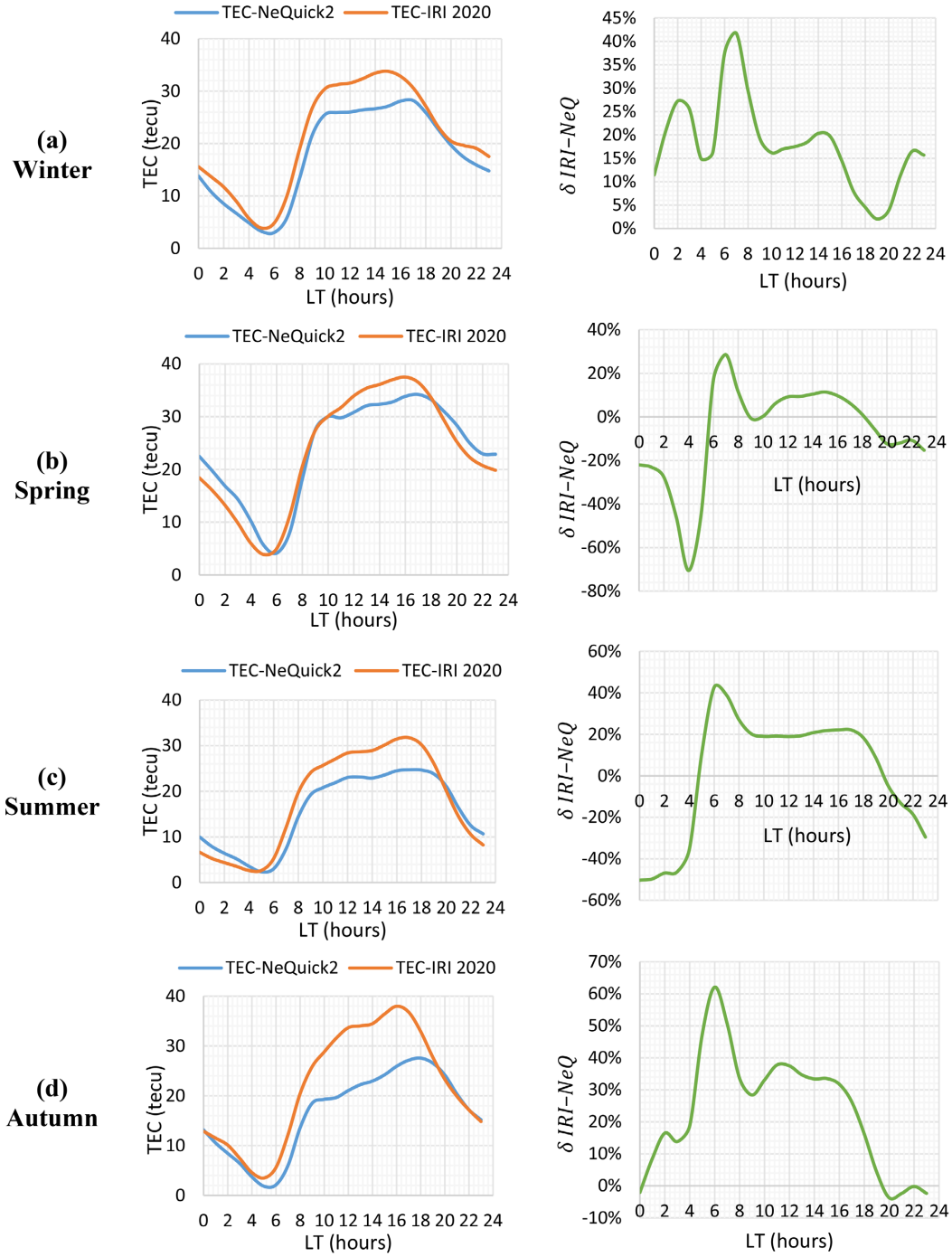


**Figure 5.** Seasonal diurnal variations of TEC by IRI-2020 and NeQuick2 according to the seasons.

predictions of the two models are similar during the night from 19:00 LT to 02:00 LT. From 03:00 LT to 18:00 LT, IRI-2020 overestimates the TEC compared to NeQuick's predictions, with a maximum discrepancy of 62.27% at 06:00 LT.

## 4. Conclusion

This work presents predictions of TEC variability at the Niamey station using the

IRI reference ionospheric model and compares these predictions with those of the NeQuick2 model. IRI-2020 modeling of TEC reveals the presence of intense counter-electrojet activity during the different solar phases and seasons. TEC variability is characterized by a trough at dawn at 05:00 LT followed by a rapid increase to a peak in the afternoon at 16:00 LT. After 16:00 LT, the TEC gradually decreases throughout the night. The trough observed at dawn is explained by a decrease in nocturnal photoionization and an increase in recombination. The rapid increase in the TEC after sunrise is linked to the increase in photoionization from solar radiation. Quantitatively, ionization increases with sunspot activity. IRI predicts the maximum TEC values at maximum phase and law values at minimum phase. The sunspots number variation during the ascending and descending phases is positive and negative, respectively. The TEC during the ascending phase is higher than during the descending phase. We have: $TEC_{Max} > TEC_{Asc} > TEC_{Desc} > TEC_{Min}$. Regarding seasonal variability, IRI predicts higher ionization in autumn and lower ionization in summer. We have: $TEC_{Aut} > TEC_{Spring} > TEC_{Win} > TEC_{Sum}$. Furthermore, TEC values are higher at the equinoxes than at the solstices, indicating a semi-annual anomaly. IRI's modeling also predicts a nighttime winter anomaly from 21:00 LT until dawn. The comparative study of the NeQuick2 model versus IRI-2020 generally shows considerable discrepancies during the day and similarities during the night. Indeed, both models predict similar nighttime TEC values in almost all solar phases and seasons. However, during the day, IRI-2020 overestimates the TEC compared to NeQuick2. Referring to IRI, it is important to improve the NeQuick model by incorporating experimental data from African equatorial stations. It should be noted that the evaluation of its ionospheric models would become more reliable by using, for example, GPS measurements or satellite data. The lack of experimental data constitutes an objective limitation of this study. We plan to evaluate the daytime performance of the IRI and NeQuick models using data measured by the SWARM satellite at the Niamey station location.

## Acknowledgements

The authors are grateful to OMNIWEB and International Service of geomagnetic indices (ISGI) for making available the sunspots number and aa index data, respectively. They also thank the IRI and NeQuick teams for making the models available.

## Conflicts of Interest

The authors declare no conflicts of interest regarding the publication of this paper.

## References

[1] Ogwala, A., Somoye, E.O., Ogunmodimu, O., Adewemimo, R.A., Onori, E.O. and Oyedokun, O. (2019) Diurnal, Seasonal and Solar Cycle Variation of Total Electron Content and Comparison with IRI-2016 Model at Birnin-Kebbi. *Annales Geophysicae*, **37**, 775-789. https://doi.org/10.5194/angeo-2018-134

[2] Liu, J., Jia, X., Zhu, Y., Xu, J., Fu, J., Zhang, R., *et al.* (2022) Comparing GNSS TEC

Data from the African Continent with IRI-2016, Iri-Plas, and Nequick Predictions. *Advances in Space Research*, **69**, 2852-2864. https://doi.org/10.1016/j.asr.2022.01.008

[3] Bilitza, D., Pezzopane, M., Truhlik, V., Altadill, D., Reinisch, B.W. and Pignalberi, A. (2022) The International Reference Ionosphere Model: A Review and Description of an Ionospheric Benchmark. *Reviews of Geophysics*, **60**, e2022RG000792. https://doi.org/10.1029/2022rg000792

[4] Nava, B., Coïsson, P. and Radicella, S.M. (2008) A New Version of the Nequick Ionosphere Electron Density Model. *Journal of Atmospheric and Solar-Terrestrial Physics*, **70**, 1856-1862. https://doi.org/10.1016/j.jastp.2008.01.015

[5] Huang, Y., Cheng, K. and Chen, S. (1989) On the Equatorial Anomaly of the Ionospheric Total Electron Content near the Northern Anomaly Crest Region. *Journal of Geophysical Research*: *Space Physics*, **94**, 13515-13525. https://doi.org/10.1029/ja094ia10p13515

[6] Rastogi, R.G. and Klobuchar, J.A. (1990) Ionospheric Electron Content within the Equatorial $F_2$ Layer Anomaly Belt. *Journal of Geophysical Research*: *Space Physics*, **95**, 19045-19052. https://doi.org/10.1029/ja095ia11p19045

[7] Kumar, S. and Singh, A.K. (2009) Variation of Ionospheric Total Electron Content in Indian Low Latitude Region of the Equatorial Anomaly during May 2007-April 2008. *Advances in Space Research*, **43**, 1555-1562. https://doi.org/10.1016/j.asr.2009.01.037

[8] Kumar, S., Singh, A.K. and Lee, J. (2014) Equatorial Ionospheric Anomaly (EIA) and Comparison with IRI Model during Descending Phase of Solar Activity (2005-2009). *Advances in Space Research*, **53**, 724-733. https://doi.org/10.1016/j.asr.2013.12.019

[9] Kumar, S. (2020) North-South Asymmetry of Equatorial Ionospheric Anomaly Computed from the IRI Model. *Annals of Geophysics*, **63**, DM330. https://doi.org/10.4401/ag-8324

[10] Sawadogo, S., Gnabahou, D.A., Pahima, T. and Ouattara, F. (2024) Solar Activity: Towards a Standard Classification of Solar Phases from Cycle 1 to Cycle 24. *Advances in Space Research*, **73**, 1041-1049. https://doi.org/10.1016/j.asr.2023.11.011

[11] Legrand, J.P. and Simon, P.A. (1989) Solar Cycle and Geomagnetic Activity: Are View for Geophysicists. Part I. The Contributions to Geomagnetic Activity of Shockwaves and of the Solar Wind. *Annals of Geophysics*, 7, 565-578.

[12] Zerbo, J.L., Amory Mazaudier, C., Ouattara, F. and Richardson, J.D. (2012) Solar Wind and Geomagnetism: Toward a Standard Classification of Geomagnetic Activity from 1868 to 2009. *Annales Geophysicae*, **30**, 421-426. https://doi.org/10.5194/angeo-30-421-2012

[13] Faynot, J.M. and Vila, P. (1979) F-Region at the Magnetic Equator. *Annals of Geophysics*, **35**, 1-19.

[14] Vassal J.A. (1982) La variation du champ magnétique et ses relations avec l'électrojet équatorial au Sénégal Oriental. *Annales de Géophysique*, **38**, 347-355. http://www.documentation.ird.fr/hor/fdi:03670

[15] Freacute deacute ric, O., Roll, and Fleury, (2011) Variability of CODG TEC and IRI 2001 Total Electron Content (TEC) during IHY Campaign Period (21 March to 16 April 2008) at Niamey under Different Geomagnetic Activity Conditions. *Scientific Research and Essays*, **6**, 3609-3622. https://doi.org/10.5897/sre10.1050

[16] Zoundi, C., Bazié, N., Kaboré, M. and Ouattara, F. (2021) Total Electron Content (TEC) Seasonal Variability under Fluctuating Activity, from 2000 to 2002, at Niamey Station. *International Journal of Physical Sciences*, **16**, 138-145. https://doi.org/10.5897/ijps2021.4960

[17] Patel, N.C., Karia, S.P. and Pathak, K.N. (2017) GPS-TEC Variation during Low to High Solar Activity Period (2010-2014) under the Northern Crest of Indian Equatorial Ionization Anomaly Region. *Positioning*, **8**, 13-35. https://doi.org/10.4236/pos.2017.82002

[18] Hajra, R., Chakraborty, S.K., Tsurutani, B.T., DasGupta, A., Echer, E., Brum, C.G.M., *et al.* (2016) An Empirical Model of Ionospheric Total Electron Content (TEC) near the Crest of the Equatorial Ionization Anomaly (EIA). *Journal of Space Weather and Space Climate*, **6**, A29. https://doi.org/10.1051/swsc/2016023

[19] Titheridge, J.E. (1973) The Electron Content of the Southern Mid-Latitude Ionosphere, 1965-1971. *Journal of Atmospheric and Terrestrial Physics*, **35**, 981-1001. https://doi.org/10.1016/0021-9169(73)90077-9

[20] Huang, Y. and Cheng, K. (1996) Solar Cycle Variations of the Equatorial Ionospheric Anomaly in Total Electron Content in the Asian Region. *Journal of Geophysical Research*: *Space Physics*, **101**, 24513-24520. https://doi.org/10.1029/96ja01297

[21] Araujo-Pradere, E.A. (1997) FoF2 Frequency Bands in El Cerrillo, Mexico during Magnetically Quiet Conditions. *Revista Brasileira de Geofísica*, **15**, 161-164. https://doi.org/10.1590/s0102-261x1997000200006

[22] Zou, L., Rishbeth, H., Müller-Wodarg, I.C.F., Aylward, A.D., Millward, G.H., Fuller-Rowell, T.J., *et al.* (2000) Annual and Semiannual Variations in the Ionospheric F2-Layer. I. Modelling. *Annales Geophysicae*, **18**, 927-944. https://doi.org/10.1007/s00585-000-0927-8

[23] Rishbeth, H., Müller-Wodarg, I.C.F., Zou, L., Fuller-Rowell, T.J., Millward, G.H., Moffett, R.J., *et al.* (2000) Annual and Semiannual Variations in the Ionospheric F2-Layer: II. Physical Discussion. *Annales Geophysicae*, **18**, 945-956. https://doi.org/10.1007/s00585-000-0945-6

[24] Ouattara, F., Zerbo, J.L., Kaboré, M. and Fleury, R. (2017) Investigation on Equinoctial Asymmetry Observed in Niamey Station Center for Orbit Determination in Europe Total Electron Content (CODG TEC) Variation during ~ Solar Cycle 23. *International Journal of Physical Sciences*, **12**, 308-321. https://doi.org/10.5897/ijps2017.4684

[25] Oryema, B., Jurua, E., D'ujanga, F.M. and Ssebiyonga, N. (2015) Investigation of TEC Variations over the Magnetic Equatorial and Equatorial Anomaly Regions of the African Sector. *Advances in Space Research*, **56**, 1939-1950. https://doi.org/10.1016/j.asr.2015.05.037

[26] Fejer, B.G. (1981) The Equatorial Ionospheric Electric Fields. a Review. *Journal of Atmospheric and Terrestrial Physics*, **43**, 377-386. https://doi.org/10.1016/0021-9169(81)90101-x

[27] Farley, D.T., Bonelli, E., Fejer, B.G. and Larsen, M.F. (1986) The Prereversal Enhancement of the Zonal Electric Field in the Equatorial Ionosphere. *Journal of Geophysical Research*: *Space Physics*, **91**, 13723-13728. https://doi.org/10.1029/ja091ia12p13723

[28] Kelley, M.C. (2009) The Earth's Ionosphere: Plasma Physics and Electrodynamics. 2nd Edition, Academic Press.

[29] Balan, N., Otsuka, Y., Bailey, G.J. and Fukao, S. (1998) Equinoctial Asymmetries in the Ionosphere and Thermosphere Observed by the MU Radar. *Journal of Geophysical Research*: *Space Physics*, **103**, 9481-9495. https://doi.org/10.1029/97ja03137

[30] Rishbeth, H., Heelis, R.A. and Müller-Wodarg, I.C.F. (2004) Variations of Thermospheric Composition According to AE-C Data and CTIP Modelling. *Annales Geo-*

*physicae*, **22**, 441-452. https://doi.org/10.5194/angeo-22-441-2004

[31] Yu, T., Wan, W., Liu, L. and Zhao, B. (2004) Global Scale Annual and Semi-Annual Variations of Daytime NmF2 in the High Solar Activity Years. *Journal of Atmospheric and Solar-Terrestrial Physics*, **66**, 1691-1701. https://doi.org/10.1016/j.jastp.2003.09.018